Parabolic quasi-Sturmian approach to proton-impact ionization of helium

A. S. Zaytsev, D. S. Zaytseva, and S. A. Zaytsev
Pacific National University, Khabarovsk 680035, Russia

L. U. Ancarani
Université de Lorraine, CNRS, LPCT, 57000 Metz, France

K. A. Kouzakov ⊙
*Department of Nuclear Physics and Quantum Theory of Collisions, Faculty of Physics,
Lomonosov Moscow State University, Moscow 119991, Russia*

A method for calculating ion-atom ionizing collisions is formulated and applied to single ionization of helium induced by energetic proton impact. Within the frozen-core model for the residual helium ion, the four-body problem in the exit channel is recast as an inhomogeneous Schrödinger equation for the Coulomb three-body system (e^-, He^+, p^+). The asymptotic behavior of its solution contains the transition amplitude. We suggest to solve the driven equation in the representation of so-called parabolic convoluted quasi-Sturmian (CQS) basis functions which are constructed using quasi-Sturmians (QSs) for the (e^-, He^+) and (p^+, He^+) subsystems. By applying the corresponding Coulomb Green's function operators, these QSs are generated from orthogonal complements to square-integrable (L^2) Sturmian functions in parabolic coordinates. In the proposed parabolic CQS approach explicit asymptotic expressions for the basis functions provide an expansion of the transition amplitude in terms of "basis amplitudes," which we express analytically. The proton-electron interaction is treated as a perturbation and is approximated by a truncated Sturmian basis-set expansion. It is found that, at least in the high-energy limit, the ionization amplitude converges pretty fast as the number of terms in the separable expansion for the proton-electron potential is increased. The calculated fully differential cross sections for singly ionizing 1-MeV p-He collisions in several kinematical regimes in the scattering plane are found to be in reasonable agreement with experimental data and with the theoretical results obtained using the first Born approximation, the 3C model, and the wave-packet convergent close-coupling method. The theory-experiment discrepancy over the binary peak position observed by other authors remains unexplained.

I. INTRODUCTION

Fully differential cross sections (FDCSs) for the ionization of helium by fast proton impact provide valuable detailed information about the dynamics of breakup processes of few-body Coulomb systems. Using cold target recoil ion momentum spectroscopy (COLTRIMS) [1–3], FDCSs of singly ionizing 1-MeV p-He collisions have been measured in various kinematical regimes [4,5]. The collected high-precision angular data stimulated several theoretical studies. The first Born approximation (FBA) with respect to the proton-helium interaction [4,5], being applied to the analysis of the experimental data, revealed shortcomings of the method, especially in the kinematic regime far from the Bethe ridge. The data were also analyzed with more advanced and involved approaches. For example, the classical trajectory Monte Carlo (CTMC) method has been applied [6]; this nonrelativistic nonperturbative approach provides a classical description of the dynamics of the three-body breakup processes, which necessarily misses some quantum mechanical effects. The

well-known continuum distorted-wave–eikonal initial-state (CDW-EIS) model [7,8] and its variations in the semiclassical and fully quantum formulations have been used [9–11]; in this model the relative motion of the proton and helium nucleus is described within the straight-line version of the impact parameter approximation, while the initial bound and final ionized electron states are treated using the distortion factors due to the two-center field of the projectile and target. The special case of the quantum CDW-EIS, the so-called 3C (or BBK) model [12,13], in which the final-state interactions in the system (e^-, He^+, p^+) are described by three Coulomb continuum functions (with, in general, effective charges), has been applied to the calculation of FDCS in Refs. [5,14]. In addition, in Ref. [5], the Born-Faddeev approximation was examined. A more advanced semiclassical approach (beyond the perturbative model), called the wave-packet convergent close-coupling (WP-CCC) method [15,16], was also implemented to compute FDCSs. Within this method the helium nucleus is assumed to be located at the origin, while the proton is assumed to be moving along the straight-line trajectory. The

electronic part of the wave function in a combined potential of the projectile and target (in the framework of the frozen-core approximation) is expanded in terms of bound states and wave-packet pseudostates describing the active electron of the helium atom (these wave-packet pseudostates represent a finite interval of the active electron continuum). The time-dependent Schrödinger equation for the total scattering wave function is then solved using a semiclassical approximation.

In spite of these theoretical developments, none of the approaches is capable of completely explaining the experimentally observed angular distributions. Specifically, the FBA reproduces the two-peak structure of the measured FDCSs in the scattering plane, with the angular positions of the binary and recoil peaks coinciding with the $\mathbf{q}$ and $-\mathbf{q}$ directions, respectively, where $\mathbf{q}$ is the momentum transfer. In the measurements, the positions of both peaks turn out to be visibly shifted towards the forward direction compared to the FBA predictions. Only a small portion of such shifts are explained by beyond-FBA theoretical approaches. The most problematic aspect is that the discrepancy between theory and experiment in the kinematical regime far off the Bethe ridge still remains in the position of the binary peak. This peak originates from the binary encounter between the projectile proton and the target electron, constituting the major ionization mechanism and giving the dominant contribution to the cross section. Therefore it is disturbing that well-established theories fail to give a proper account of the experimentally observed binary peak position. This points out the need for further development of our theoretical understanding of ion-atom ionizing collisions in particular, and the Coulomb few-body problem in general. The refinement of the corresponding theoretical apparatus is also important for such applications as radiation material science [17] and ion therapy [18,19], where the ion-atom ionizing collisions play one of the key roles.

In this paper, we wish to investigate the ionization process under consideration with our quantum approach outlined in Ref. [20] that accounts for the total energy spectrum of the active electron. The scope here is twofold. The first, methodological, aim is to provide the analytical details of the method, together with the implemented numerical strategy, and to test its robustness and efficiency in various kinematic situations. The second aim is to find out whether the proposed approach can provide an overall better description of the measured angular data, and in particular if it can help in shedding some light on the origin of the binary peak position discrepancy. Since we are dealing with high-energy protons, their plane-wave boundary conditions are conveniently described in parabolic coordinates with the axis $\hat{z}$ chosen along the incident proton momentum $\mathbf{K}_0$. Our treatment of the transition amplitude assumes that the state of the residual He$^+$ ion is frozen in the exit channel of the ionization reaction and therefore the calculation of the amplitude is cast as an inhomogeneous Schrödinger equation for the Coulomb three-body system (e^-, He^+, p^+): the asymptotic behavior of its solution contains the sought-for amplitude. We propose to solve this driven equation by expanding in convolutions of adequate quasi-Sturmian functions corresponding to the two (e^-, He^+) and (p^+, He^+) subsystems. In doing this, we introduce an auxiliary proton plane wave (with a momentum $Q \lesssim K_0$) into the basis functions in order to avoid numerical evaluations of

the integrals of very rapidly oscillating functions. The proton-electron interaction, treated as a perturbation, is approximated by a truncated expansion on the basis of square-integrable (L^2) Sturmian functions in parabolic coordinates. The efficiency of such a representation of the Coulomb potential is tested in the high-energy limit, in particular by comparing the calculated cross sections with the results obtained in the framework of the 3C model [14], which obeys correct leading-order Coulomb asymptotic conditions.

The paper is organized as follows. In Sec. II A, within the frozen-core model for the residual helium ion the ionization problem is cast in the form of a driven equation. In Sec. II B, we discuss the details of constructing the parabolic convoluted quasi-Sturmian (CQS) functions from one-particle quasi-Sturmians (QSs). For the latter we derive analytically the leading asymptotic behavior and identify what we name *basis amplitudes*. The solution of the driven equation is then proposed as an expansion on CQS: from the asymptotic analysis, the transition amplitude to the ionization process is finally expressed in terms of these basis amplitudes. In Secs. II C and II D we use finite Sturmian-expansion representations of the proton-electron interaction and Green's function of the two noninteracting hydrogenlike subsystems (e^-, He^+) and (p^+, He^+) to convert the driven equation into a matrix equation. The numerical solution of the algebraic problem provides then the coefficients of the CQS expansion. In Sec. III, the results of our numerical calculations are presented. First, we examine convergence issues of the differential ionization cross sections, in particular with respect to the number of terms in the representation of the proton-electron potential. Then, we make a comparison with the experimental data and theoretical cross sections obtained by other authors. Finally, Sec. IV provides a summary of this work.

Atomic units (a.u.) in which $\hbar = e = m_e = 1$ are used throughout unless otherwise specified.

II. THEORY

We wish to describe the ionization of helium in its ground state by energetic proton impact,

$$\text{He}(1s^2) + p^+ \rightarrow e^- + p^+ + \text{He}^+(1s), \tag{1}$$

leaving the target in the hydrogenic ground state $\psi_{1s}^{\text{He}^+}$.

A. Transition amplitude

Using the frozen-core model for the residual helium ion, we have a factorized final-state wave function of the form

$$\Psi_{\mathbf{K},\mathbf{k}_e}^{(-)}(\mathbf{R}, \mathbf{r})\psi_{1s}^{\text{He}^+}(\mathbf{r}'), \tag{2}$$

$\mathbf{r}$, $\mathbf{r}'$, and $\mathbf{R}$ being the electrons and the proton coordinates with respect to the origin (the helium nucleus), and

$$\psi_{1s}^{\text{He}^+}(\mathbf{r}') = \sqrt{8/\pi} \exp(-2r') \tag{3}$$

is the frozen electron wave function. Assuming this, we can then write down the following expression for the amplitude:

$$T_{\mathbf{K},\mathbf{k}_e} = \langle \Psi_{\mathbf{K},\mathbf{k}_e}^{(-)}, \psi_{1s}^{\text{He}^+} | \hat{V}_i | \mathbf{K}_0, \Phi^{(0)} \rangle. \tag{4}$$

Denoting $\hat{H}$ the Hamiltonian of the three-body system (e^-, He^+, p^+), the final-state wave function $\Psi_{\mathbf{K},\mathbf{k}_e}^{(-)}$ satisfies the

Schrödinger equation

$$[E - \hat{H}]|\Psi_{\mathbf{K},\mathbf{k}_e}^{(-)}\rangle = 0, \tag{5}$$

where $\mathbf{k}_e$ and $\mathbf{K}$ are the momenta of the electron and proton, respectively. Assuming the helium nucleus to be at rest during the process, the energy of the system is given by $E = \frac{k_e^2}{2} + \frac{K^2}{2m_p}$ ($m_p \simeq 1836.15$ is the mass of the proton).

In the amplitude (4), $\hat{V}_i$ is the incident channel interaction:

$$V_i = \frac{2}{R} - \frac{1}{|\mathbf{R} - \mathbf{r}|} - \frac{1}{|\mathbf{R} - \mathbf{r}'|}. \tag{6}$$

Let F denote the matrix element

$$F(\mathbf{R}, \mathbf{r}) = \langle \psi_{1s}^{\mathrm{He}^+} | \hat{V}_i | \Phi^{(0)} \rangle, \tag{7}$$

where the correlated ground-state wave function $\Phi^{(0)}(\mathbf{r}, \mathbf{r}')$ is obtained by diagonalizing of the full helium Hamiltonian (see details in Sec. III). The amplitude, symmetrized in the coordinates $\mathbf{r}$ and $\mathbf{r}'$ of the two target electrons, then reads

$$T_{\mathbf{K},\mathbf{k}_e}^S = \sqrt{2}\langle \Psi_{\mathbf{K},\mathbf{k}_e}^{(-)} | \mathbf{K}_0, F \rangle, \tag{8}$$

where $|\mathbf{K}_0\rangle$ denotes the plane wave

$$\langle \mathbf{R} | \mathbf{K}_0 \rangle = e^{i\mathbf{K}_0 \cdot \mathbf{R}} \tag{9}$$

for the projectile with the momentum $\mathbf{K}_0$.

It follows from the property of the Green's function operator $\hat{G}^{(+)}(E) \equiv [E - \hat{H}]^{-1}$ [21,22] that the sought-for amplitude is contained in the leading asymptotic form—for large values of the hyperradius $\rho = \sqrt{m_p R^2 + r^2}$—of the solution of the inhomogeneous equation [20]

$$[E - \hat{H}]|\Phi^{(+)}\rangle = |\mathbf{K}_0, F\rangle, \tag{10}$$

satisfying outgoing boundary conditions. Indeed, the solution can be formally written as

$$|\Phi^{(+)}\rangle = \hat{G}^{(+)}(E)|\mathbf{K}_0, F\rangle. \tag{11}$$

In order to make this formal approach numerically practical, we use parabolic quasi-Sturmians described hereafter to search the solution $\Phi^{(+)}$ of Eq. (10), and from its asymptotic behavior we extract the transition amplitude.

B. One-particle parabolic quasi-Sturmians and two-particle convoluted quasi-Sturmians

The final channel Hamiltonian $\hat{H}$ for the three-body system can be written as

$$\hat{H} = \hat{H}_0 + \hat{U}, \tag{12}$$

where we have a separable three-body Hamiltonian

$$\hat{H}_0 = -\frac{1}{2m_p}\nabla_{\mathbf{R}}^2 - \frac{1}{2}\nabla_{\mathbf{r}}^2 + \frac{1}{R} - \frac{1}{r}, \tag{13}$$

and the proton-electron interaction identified as the perturbation

$$\hat{U} = -\frac{1}{|\mathbf{R} - \mathbf{r}|}. \tag{14}$$

If desired, the splitting (12) of the Hamiltonian can be refined by including in $\hat{H}_0$ also short-range corrections, for example by using Hartree potentials as done in Ref. [20].

In this work we treat the problem in parabolic coordinates (ξ, η, ϕ) with the $\hat{z}$ axis chosen along the incident proton momentum $\mathbf{K}_0$, and we use the square-integrable Sturmians defined by [23]

$$\langle \xi, \eta, \phi | n, m, \varkappa \rangle = \frac{e^{i\varkappa\phi}}{\sqrt{2\pi}} \varphi_n^{|\varkappa|}(\xi)\, \varphi_m^{|\varkappa|}(\eta), \tag{15}$$

where

$$\varphi_n^\lambda(\rho) = \sqrt{\frac{2bn!}{(n+\lambda)!}}\,(2b\rho)^{\lambda/2}e^{-b\rho}L_n^\lambda(2b\rho), \quad \lambda = |\varkappa|, \tag{16}$$

with the basis scale parameter b; L_n^λ are the associated Laguerre polynomials [24].

Let

$$|\mathfrak{N}\rangle \equiv |\mathfrak{n}\rangle|\mathfrak{m}\rangle \tag{17}$$

be the product of two Sturmians

$$|\mathfrak{n}\rangle \equiv |n_1, n_2, \varkappa\rangle, \quad |\mathfrak{m}\rangle \equiv |m_1, m_2, \omega\rangle, \tag{18}$$

of the parabolic coordinates ξ_1, η_1, ϕ_1 and ξ_2, η_2, ϕ_2 associated with $\mathbf{R}$ and $\mathbf{r}$, respectively. Note that $\omega = -\varkappa$ since we restrict ourselves to the states with the magnetic quantum number $M_L = 0$. Let

$$|\widetilde{\mathfrak{l}}\rangle = |\widetilde{n, m, \varkappa}\rangle = w|n, m, \varkappa\rangle, \quad w(\xi, \eta) = \frac{4}{\xi + \eta}, \tag{19}$$

be the vector orthogonal to $|\mathfrak{l}\rangle \equiv |n, m, \varkappa\rangle$, that is to say,

$$\langle \widetilde{n, m, \varkappa} | n', m', \varkappa' \rangle = \delta_{n,n'}\delta_{m,m'}\delta_{\varkappa,\varkappa'}. \tag{20}$$

Then $|\widetilde{\mathfrak{N}}\rangle \equiv |\widetilde{\mathfrak{n}}\rangle|\widetilde{\mathfrak{m}}\rangle$ represents the orthogonal complement to $|\mathfrak{N}\rangle$ [20], such that

$$\langle \mathfrak{N} | \widetilde{\mathfrak{N}'} \rangle = \delta_{\mathfrak{N},\mathfrak{N}'}, \tag{21}$$

$\mathfrak{N}$ denoting the set of quantum numbers $\mathfrak{N} \equiv \{\mathfrak{n}, \mathfrak{m}\}$.

We suggest for the solution to the driven Eq. (10) an expansion

$$|\Phi^{(+)}\rangle = \sum_{\mathfrak{N}} C_{\mathfrak{N}}|\mathcal{S}_{\mathbf{Q},\mathfrak{N}}^{(+)}\rangle \tag{22}$$

in terms of functions $\mathcal{S}_{\mathbf{Q},\mathfrak{N}}^{(+)}$ satisfying the equation

$$[E - \hat{H}_0]|\mathcal{S}_{\mathbf{Q},\mathfrak{N}}^{(+)}\rangle = |\mathbf{Q}, \widetilde{\mathfrak{N}}\rangle, \tag{23}$$

that is similar to Eq. (10) with $\mathbf{Q} = \varepsilon\mathbf{K}_0$, $\varepsilon < 1$.

The formal separability of Eq. (23) is based on treating the proton-electron Coulomb interaction as a perturbation. On the other hand, the solution of Eq. (23) can be expressed in terms of basis functions that we call *convoluted* quasi-Sturmians [25]: they are constructed as a convolution of two suited one-particle parabolic QSs (see, e.g., Eq. (26) in Ref. [23]), corresponding to the noninteracting hydrogenlike systems, (p^+, He$^+$) and (e^-, He$^+$). For the present purposes, we need to include also an auxiliary plane-wave $|\mathbf{Q}\rangle$ state for the projectile, so that we modify the one-particle QS introduced in Ref. [23]. These "shifted" QSs, for given charge Z and mass M, are defined by

$$|\mathcal{Q}_{\mathbf{Q},\mathfrak{l}}^{(+)}\rangle = \hat{G}_C^{(+)}(Z, M; \mathcal{E})|\mathbf{Q}\rangle|\widetilde{\mathfrak{l}}\rangle, \tag{24}$$

where $\hat{G}_C^{(+)}(Z, M; \mathcal{E}) = [\mathcal{E} - \hat{H}_C]^{-1}$ represents the Coulomb Green's function for the Hamiltonian

$$\hat{H}_C = -\frac{1}{2M}\nabla_{\mathbf{X}}^2 + \frac{Z}{X}, \tag{25}$$

X being the position vector.

Since in our approach the transition amplitude is eventually extracted from the asymptotic behavior of solution (22), we need the asymptotic behavior of $|\mathcal{Q}_{\mathbf{Q},\mathfrak{l}}^{(+)}\rangle$ for large X. We were

able to show that (see Appendix A for details of the derivation)

$$\langle \mathbf{X} | \mathcal{Q}_{\mathbf{Q},\mathfrak{l}}^{(+)}\rangle \simeq -M \frac{e^{i\varkappa\phi}}{\sqrt{2\pi}} \mathcal{A}_{\mathfrak{l}}^{(+)}(\beta, P, Q; \theta)$$

$$\times \frac{\exp\{i[PX - \beta\ln(2PX)]\}}{X}, \tag{26}$$

where $P = \sqrt{2M\mathcal{E}}$ and $\beta = \frac{MZ}{P}$ is the Sommerfeld parameter; θ, ϕ are the polar angles of **X**. The amplitude $\mathcal{A}_{\mathfrak{l}}^{(+)}$ is expressed as

$$\mathcal{A}_{\mathfrak{l}}^{(+)}(\beta, P, Q; \theta) = \frac{i}{P}\sqrt{\frac{n!m!}{(n+\lambda)!(m+\lambda)!}}\left[\frac{1+(p+q)}{1-(p-q)}\frac{1}{c^2+\alpha s^2}\right]^{i\beta} e^{-\frac{\pi\beta}{2}}$$

$$\times \left[\frac{4p}{1-(p-q)^2}\frac{1}{c^2+\alpha s^2}\right]^{1+\lambda}\left(\frac{\sin\theta}{2}\right)^{\lambda}\left[-\frac{1-(p+q)}{1+(p+q)}\right]^n\left[-\frac{1-(p-q)}{1+(p-q)}\right]^m$$

$$\times \sum_{\nu=0}^{n}\sum_{\mu=0}^{m}c_{\nu}^{(n,\lambda)}c_{\mu}^{(m,\lambda)}\Gamma(i\beta+\lambda+\nu+\mu+1)\left[\frac{-4p}{[1-(p+q)][1-(p-q)]}\frac{1}{c^2+\alpha s^2}\right]^{\nu+\mu}(c^2)^{\nu}(\alpha s^2)^{\mu}, \tag{27}$$

with

$$p = -\frac{iP}{2b}, \quad q = -\frac{iQ}{2b}, \quad \alpha = \frac{1-(p+q)^2}{1-(p-q)^2},$$

$$c = \cos\frac{\theta}{2}, \quad s = \sin\frac{\theta}{2}. \tag{28}$$

Here, $\lambda = |\varkappa|$, and

$$c_{\nu}^{(n,\lambda)} = (-1)^{\nu}\frac{(n+\lambda)!}{(n-\nu)!(\nu+\lambda)!\nu!} \tag{29}$$

represent the coefficients of the expansion

$$L_n^{\lambda}(x) = \sum_{\nu=0}^{n}c_{\nu}^{(n,\lambda)}x^{\nu}. \tag{30}$$

When $Q = 0$, results (26) and (27) reduce to the formulas presented in Ref. [23] (note, however, a sign difference since $\hat{G}_C^{(\pm)} = [\hat{H}_C - \mathcal{E}]^{-1}$ was used in Ref. [23]).

Finally, comparing the large-ρ asymptotic behavior of Eq. (11), that is to say, the solution $|\Phi^{(+)}\rangle$ of the inhomogeneous Eq. (10), and that of

$$|\mathcal{S}_{\mathbf{Q},\mathfrak{N}}^{(+)}\rangle = \hat{G}_0^{(+)}(E)|\mathbf{Q}, \tilde{\mathfrak{N}}\rangle, \tag{31}$$

where $\hat{G}_0^{(+)}(E) = [E - \hat{H}_0]^{-1}$, we can deduce the transition amplitude $T_{\mathbf{K},\mathbf{k}_e}^S$. Up to a phase factor, including the logarithmic one that corresponds to the Coulomb proton-electron interaction, the amplitude is expressed in terms of the coefficients $C_{\mathfrak{N}}$ of expansion (22), as [20]

$$T_{\mathbf{K},\mathbf{k}_e}^S = \sqrt{2}2\pi\sum_{\mathfrak{N}}C_{\mathfrak{N}}e^{i\varkappa(\phi_p-\phi_e)}\mathcal{A}_{\mathfrak{n}}^{(+)}(\beta_p, K, Q; \theta_p)$$

$$\times \mathcal{A}_{\mathfrak{m}}^{(+)}(\beta_e, k_e, 0; \theta_e), \tag{32}$$

where $\beta_p = \frac{m_p}{K}$ and $\beta_e = -\frac{1}{k_e}$ are the Sommerfeld parameters for the two subsystems (p^+, He^+) and (e^-, He^+). A remarkable feature of this result is that the angular dependence of the

transition amplitude is found only in $\mathcal{A}_{\mathfrak{n}}^{(+)}$ and $\mathcal{A}_{\mathfrak{m}}^{(+)}$, quantities that we name *basis amplitudes*.

C. Matrix equation for the coefficients $C_{\mathfrak{N}}$

Inserting expansion (22) into Eq. (10), and using Eq. (31), gives

$$\sum_{\mathfrak{N}'}[|\mathbf{Q}, \tilde{\mathfrak{N}}'\rangle - \hat{U}\,\hat{G}_0^{(+)}(E)|\mathbf{Q}, \tilde{\mathfrak{N}}'\rangle]\,C_{\mathfrak{N}'} = \hat{V}|\mathbf{K}_0, f\rangle. \tag{33}$$

Then, projecting this equation by $\langle\mathbf{Q}, \mathfrak{N}|$, and inserting the unit operator

$$\hat{I} = \sum_{\mathfrak{M}}|\mathfrak{M}\rangle\langle\tilde{\mathfrak{M}}|, \tag{34}$$

we obtain the following matrix equation:

$$\sum_{\mathfrak{N}'}\left[\delta_{\mathfrak{N},\mathfrak{N}'} - \sum_{\mathfrak{M}}\langle\mathfrak{N}|\hat{U}|\mathfrak{M}\rangle\langle\mathbf{Q}, \tilde{\mathfrak{M}}|\hat{G}_0^{(+)}(E)|\mathbf{Q}, \tilde{\mathfrak{N}}'\rangle\right]$$

$$\times C_{\mathfrak{N}'} = D_{\mathfrak{N}}, \tag{35}$$

where

$$D_{\mathfrak{N}} \equiv \langle\mathfrak{N}|\mathbf{K}_0 - \mathbf{Q}, F\rangle. \tag{36}$$

In the numerical implementation of our approach the operator $\hat{U}$ is approximated by the truncated representation

$$\hat{U}^{\mathcal{N}_0} = \sum_{\mathfrak{N},\mathfrak{M}}|\tilde{\mathfrak{N}}\rangle\langle\mathfrak{N}|\hat{U}|\mathfrak{M}\rangle\langle\tilde{\mathfrak{M}}|, \tag{37}$$

in the "inner" subset of the basis (17) whose size $\mathcal{N}_0 = (2M_0 + 1)N_0^4$ is determined by the limits M_0 and N_0 to the ranges $|\varkappa| \leqslant M_0$ and $n_j, m_j < N_0$ $(j = 1, 2)$. Thus, the infinite-matrix problem (35) reduces to a finite system of algebraic equations for the "inner" coefficients $C_{\mathfrak{N}}$ (with $\mathfrak{N}$ labeling the "inner" subset vectors), whereas the corresponding "outer" coefficients $C_{\mathfrak{N}}$ coincide with $D_{\mathfrak{N}}$ given by Eq. (36).
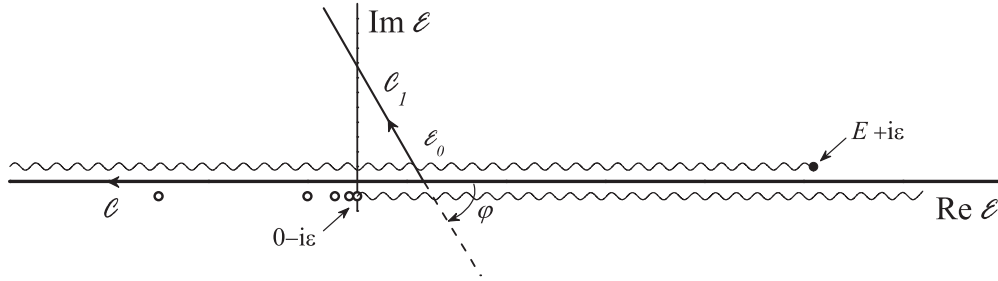
FIG. 1. The contour $\mathcal{C}$ goes from ∞ to $-\infty$ just above the real axis. The integration path $\mathcal{C}_1$ in Eq. (39) is obtained by a negative angle φ rotation of $\mathcal{C}$, about some point $\mathcal{E}_0$ on the positive real axis. The bound-state poles of $\hat{G}_C^{(+)}(-1, 1; \mathcal{E})$ are shown by open circles. The unitarity branch cuts of $\hat{G}_C^{(+)}(-1, 1; \mathcal{E})$ and $\hat{G}_C^{(+)}(1, m_p; E - \mathcal{E})$ are depicted by the wavy lines lying beneath and above the contour $\mathcal{C}$, respectively.

Note that the "outer" coefficients appear on the right-hand side of the resulting system due to the second term on the left-hand side of Eq. (35).

D. Green's function matrix elements

In matrix equation (35) we need the Green's function operator $\hat{G}_0^{(+)}$ matrix elements. For their evaluation we use the representation in the form of a convolution integral (see, e.g., Refs. [26,27]):

$$\hat{G}_0^{(+)}(E) = \frac{1}{2\pi i} \int_{\mathcal{C}} d\mathcal{E} \, \hat{G}_C^{(+)}(-1, 1; \mathcal{E}) \hat{G}_C^{(+)}(1, m_p; E - \mathcal{E}). \tag{38}$$

Instead of the contour $\mathcal{C}$, which runs just above the unitary cut and bound-state poles of $\hat{G}_C^{(+)}(-1, 1; \mathcal{E})$, we integrate along

a path $\mathcal{C}_1$ obtained by rotation of the contour $\mathcal{C}$, about some point $\mathcal{E}_0$ on the positive real energy axis through a negative angle φ (see Fig. 1) [27]. Thus, on the contour $\mathcal{C}_1$ the integration variable is set to $\mathcal{E} = \mathcal{E}_0(1 + te^{i\varphi})$ where t runs from ∞ to $-\infty$. Explicitly we write

$$\langle \mathbf{Q}, \tilde{\mathfrak{N}} | \hat{G}_0^{(+)}(E) | \mathbf{Q}, \tilde{\mathfrak{N}}' \rangle = \frac{1}{2\pi i} \int_{\mathcal{C}_1} d\mathcal{E} \langle \tilde{\mathfrak{m}} | \hat{G}_C^{(+)}(-1, 1; \mathcal{E}) | \tilde{\mathfrak{m}}' \rangle$$
$$\times \langle \tilde{\mathfrak{n}} | \langle \mathbf{Q} | \hat{G}_C^{(+)}(1, m_p; E - \mathcal{E}) | \mathbf{Q} \rangle | \tilde{\mathfrak{n}}' \rangle. \tag{39}$$

It turns out that both factors in the integrand can be expressed analytically, as a finite summation involving Gauss hypergeometric functions $_2F_1$ [24]. The useful formula reads (the derivation is given in Appendix B):

$$\langle \tilde{l} | \langle \mathbf{Q} | \hat{G}_C^{(+)}(Z, M; \mathcal{E}) | \mathbf{Q} \rangle | \tilde{l}' \rangle = -\delta_{\varkappa, \varkappa'} \frac{2iM}{P}(1 - \zeta)(-\chi)^{n'+m}(-\delta)^{n+m'} \sqrt{\binom{n + \lambda}{n} \binom{m + \lambda}{m} \binom{n' + \lambda}{n'} \binom{m' + \lambda}{m'}}$$

$$\times \sum_{\ell=0}^{u+v} c_\ell \, \zeta^{-\ell} \, \frac{\Gamma(\lambda + \ell + 1 + i\beta)\Gamma(L + 1 - 2\ell)}{\Gamma(L + \lambda + 2 - \ell + i\beta)}$$

$$\times \, _2F_1(L - 2\ell + 1, -\lambda - \ell + i\beta; L + \lambda + 2 - \ell + i\beta; \zeta). \tag{40}$$

Here $P = \sqrt{2M\mathcal{E}}$, $\beta = \frac{MZ}{P}$, $\lambda = |\varkappa|$, $L = n + m + n' + m'$, and the coefficients c_ℓ are

$$c_\ell = \sum_{j=\max(\ell-v,0)}^{\min(\ell,u)} \frac{\binom{m_1}{j}\binom{m_1'}{j}\binom{m_2}{\ell-j}\binom{m_2'}{\ell-j}}{\binom{j+\lambda}{j}\binom{\ell-j+\lambda}{\ell-j}}, \tag{41}$$

with $u = \min(n, n')$ and $v = \min(m, m')$. The argument of $_2F_1$ is defined by

$$\zeta = \chi\delta, \quad \chi = \frac{1 - (p+q)}{1 + (p+q)}, \quad \delta = \frac{1 - (p-q)}{1 + (p-q)}, \tag{42}$$

with

$$p = -\frac{iP}{2b}, \quad q = -\frac{iQ}{2b}. \tag{43}$$

Note that when $Q = 0$, the mathematical result (40) coincides with that published in Appendix A of Ref. [23].

Setting $\mathbf{Q} = \mathbf{K}_0$ would allow us to ideally incorporate the proton plane wave into the Green's function matrix element. However, we found out that for the contour integral (39) to be

independent of the angle of rotation φ, a necessary condition is

$$E - \mathcal{E}_0 > \frac{Q^2}{2m_p}. \tag{44}$$

Note that $E - \mathcal{E}_0$ is the energy of the pair (p^+, He^+) when the energy of (e^-, He^+) is equal to $\mathcal{E}_0$.

III. RESULTS

From the CQS ionization amplitude, we calculate the FDCS which, in the laboratory frame, reads

$$\frac{d^5\sigma}{dE_e d\Omega_e d\Omega_p} = k_e \frac{m_p^2}{(2\pi)^5} \frac{K}{K_0} |T_{\mathbf{K}, \mathbf{k}_e}^S|^2. \tag{45}$$

We investigate here the coplanar geometry, and consider the kinematic conditions explored experimentally [4,5]: the incident proton energy is $E_p = 1$ MeV, the electron of the target is ejected with energies $E_e \lesssim 20$, and the momentum-transfer
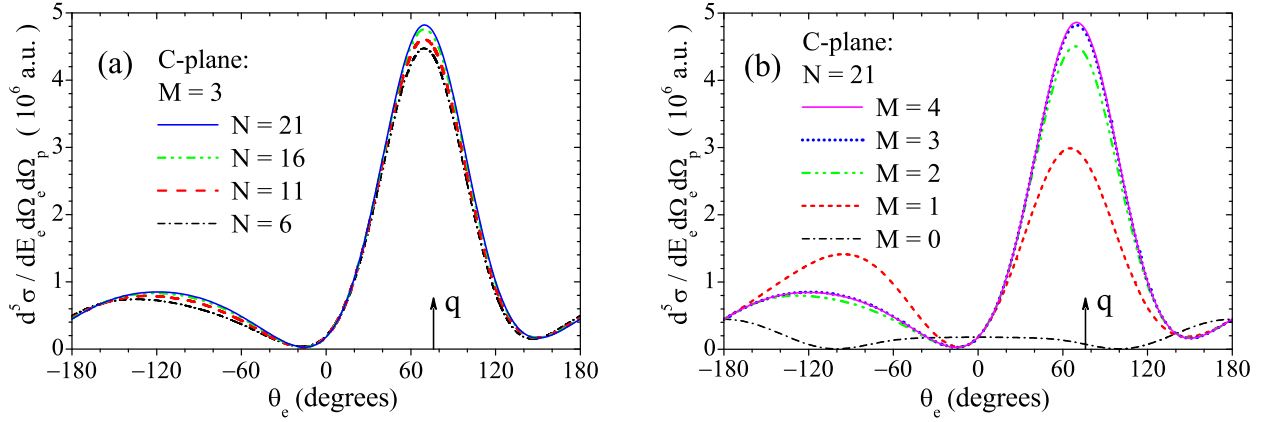
FIG. 2. Convergence behavior of the 2C-like FDCS as the upper limit: (a) N of the summation in Eq. (51) over n_j and m_j ($j = 1, 2$) is varied at fixed $M = 3$; (b) M of the summation in Eq. (51) over $\varkappa$ is varied at fixed $N = 21$. The kinematic conditions are $E_p = 1$ MeV, $E_e = 6.5$ eV, and $q = 0.75$ a.u. The arrow indicates the direction of the momentum transfer.

values are relatively small, $q \lesssim 2$ a.u. Specifically, we plot the calculated differential cross sections versus the electron scattering angle θ_e. It is well known that these FDCSs have a typical two-peak structure: a peak close to the direction of the momentum transfer $\mathbf{q} = \mathbf{K}_0 - \mathbf{K}$ (called the binary peak), and another peak close to the opposite direction (called the recoil peak).

The calculations have been carried out using a quite accurate ground-state wave function $\Phi^{(0)}(\mathbf{r}, \mathbf{r}')$ represented by an expansion

$$|\Phi^{(0)}\rangle = \sum_{\ell=0}^{\ell_{\max}} \sum_{n,n'=0}^{n_{\max}} \mathcal{C}_{n,n'}^{\ell} |n, n', \ell\rangle \qquad (46)$$

in terms of the orthonormal basis functions

$$\langle \mathbf{r}, \mathbf{r}' | n, n', \ell \rangle \equiv \frac{\chi_n^{\ell}(r) \chi_{n'}^{\ell}(r')}{r r'} \mathcal{Y}_{00}^{\ell\ell}(\hat{\mathbf{r}}, \hat{\mathbf{r}}'). \qquad (47)$$

The angular part of Eq. (47) is given by the bispherical harmonics

$$\mathcal{Y}_{LM}^{\ell\ell'}(\hat{\mathbf{r}}, \hat{\mathbf{r}}') = \sum_{m+m'=M} (\ell m \ell' m' | LM) Y_{\ell m}(\hat{\mathbf{r}}) Y_{\ell' m'}(\hat{\mathbf{r}}'), \qquad (48)$$

while the radial part consists of the square-integrable Laguerre basis functions

$$\chi_n^{\ell}(r) = \sqrt{2b_0} [(n+1)_{2\ell+2}]^{-\frac{1}{2}} (2b_0 r)^{\ell+1} e^{-b_0 r} L_n^{2\ell+2}(2b_0 r). \qquad (49)$$

The coefficients $\mathcal{C}_{n,n'}^{\ell}$ are obtained (see, e.g., Ref. [28]) by diagonalizing of the matrix of the Hamiltonian

$$\hat{H}_{\text{He}} = -\frac{1}{2}\nabla_{\mathbf{r}}^2 - \frac{1}{2}\nabla_{\mathbf{r}'}^2 - \frac{2}{r} - \frac{2}{r'} + \frac{1}{|\mathbf{r} - \mathbf{r}'|}. \qquad (50)$$

Taking up to $\ell_{\max} = 3$ and $n_{\max} = 25$, and choosing the basis parameter $b_0 = 1.688$, we obtain $E_0 = -2.9033$ a.u. for the ground-state energy. This energy is the same as the one corresponding to the bound state built and used in the ($e, 3e$) study [29], so that we can expect both initial-state descriptions to be of comparable good quality; in that reference it was shown that sufficient convergence was reached with respect to the target state. In order to further confirm this we increase $\ell_{\max}$ and $n_{\max}$ to 5 and 35, respectively. Even though the extension of

the basis set yields a better energy value ($E_0 = -2.9035$ a.u.), we have checked that this more correlated initial-state wave function does not affect the differential cross-section results [possibly for the reason that the decisive contribution comes from the basis vectors (47) with $\ell = 0$]. Note that the role played by the initial helium ground state has been investigated within the 3C model in Ref. [14]. While the level of accuracy of the corresponding wave function modifies the binary/recoil peaks ratio it does not provide any shift in their position. We should mention that the best correlated helium wave function used in the FBA and 3C calculations [14] has an energy just a little better (2.9037 a.u.).

A. Convergence tests

In order to make an estimate of the rate of convergence of the expansion (32), and determine limits M and N to the ranges $|\varkappa| \leqslant M$ and $n_j, m_j < N$, $j = 1, 2$, we take as a numerical testbed the following 2C-like model approximation
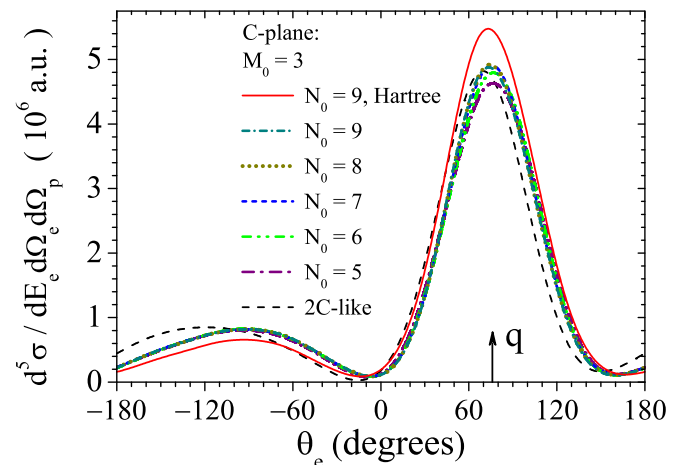

FIG. 3. Convergence behavior of FDCS as more terms are included in the Sturmian representation (37) of the proton-electron potential. The kinematic conditions are $E_p = 1$ MeV, $E_e = 6.5$ eV, and $q = 0.75$ a.u.
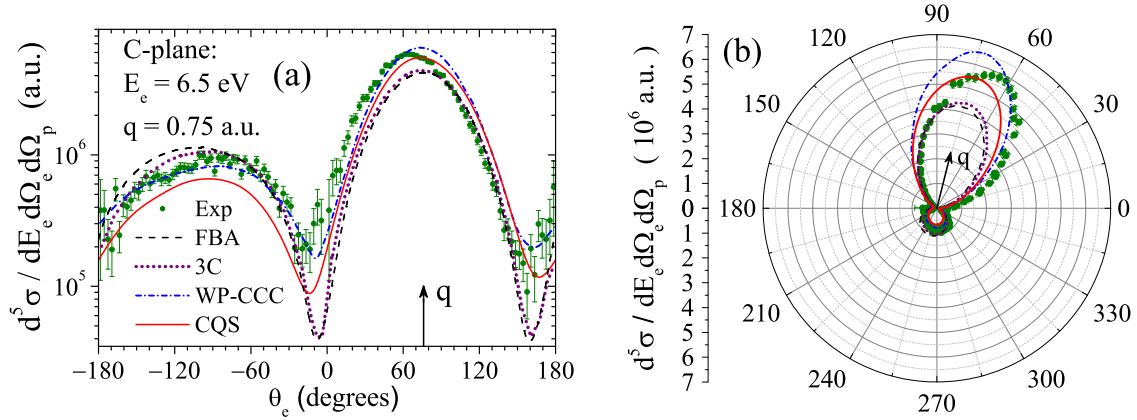
FIG. 4. FDCS for single ionization of helium by 1-MeV protons in the collision plane as a function of the ejected-electron angle. (a) The results on a logarithmic scale, and (b) the results in polar coordinates to highlight discrepancies between the theoretical and experimental electron angular distributions. The electron emission energy is $E_e = 6.5$ eV, and the total momentum transfer is $q = 0.75$ a.u. The solid curve shows the results obtained with our method of convoluted quasi-Sturmians (CQS). The experimental data are shown by solid circles with error bars, the FBA and 3C calculations (using a strongly correlated ground-state wave function of helium [30]) by dashed and dotted lines, respectively, and the dash-dotted line represents the WP-CCC results.

for the transition amplitude:

$$T_{\mathbf{K},\mathbf{k}_e}^{2C} = \sqrt{2}2\pi \sum_{\mathfrak{N}} \langle \mathfrak{N}|0,F \rangle e^{i\varkappa(\phi_p - \phi_e)}$$

$$\times \, \mathcal{A}_{\mathfrak{n}}^{(+)}(\beta_p, K, K_0; \theta_p) \, \mathcal{A}_{\mathfrak{m}}^{(+)}(\beta_e, k_e; \theta_e), \quad (51)$$

which is obtained by neglecting in Eq. (33) the operator $\hat{U}$ [see Eq. (14)]. Here we put $Q = K_0$. In all calculations, we set the basis scale parameter $b = 1$ in Eq. (16) (other values do not change substantially the numerical aspects).

We successively extended the limits of summation in Eq. (51) up to $M = 4$ and $N = 21$, and examined the FDCS convergence behavior as the number of parabolic Sturmian basis functions used to describe the driven term (33) is increased. As shown in Fig. 2 satisfactory convergence of the cross section can be achieved with $N \approx 20$. In turn, the value of M turns out to be limited due to the extremely small proton scattering angle $\theta_p = 0.0035902°$, so that convergence is observed already at $M = 3$.

Now that we have outlined the boundary for the set of basis functions involved in the transition amplitude computation, we proceed to Eq. (33) which is solved numerically using separable expansions for both $\hat{U}$ and $\hat{G}_0^{(+)}$. In order to suppress oscillations of the driven term in Eq. (33) (due to the presence of the fast projectile plane wave $|\mathbf{K}_0\rangle$), we have introduced an auxiliary proton plane wave $|\mathbf{Q}\rangle$ into the basis functions (31). While complete elimination of the rapidly oscillating factor corresponds to the case of $Q = K_0$ [see Eq. (33)], constraint (44) rules out this choice. Thus, the only way to bring Q to K_0 as close as possible is to minimize $\mathcal{E}_0$. In doing this, one should not bring $\mathcal{E}_0 > 0$ too close to the origin, since this can reduce the accuracy of the numerical computation of the Green's function matrix elements (39). In our case, the energy of the incident proton is $E_p \simeq 36749.33$ a.u., so that the total energy of the scattered proton and the ejected electron is $E = E_p + \varepsilon_0^{\text{He}} - \varepsilon_0^{\text{He}^+} \simeq 36748.42$ a.u. Then putting $\mathcal{E}_0 = E \times 10^{-5} \simeq 0.36748$ a.u. enables us to choose $Q = 0.999945K_0$ and get the value 0.63893 a.u. for the difference $K_0 - Q$.

The convergence behavior of the transition amplitude (32) is also examined as the number of terms in the representation (37) of the proton-electron potential is increased. Specifically, based on the above convergence study of the 2C-like amplitude (51), we put $M_0 = 3$. As shown in Fig. 3, the convergence of the cross section is achieved at $N_0 = 9$. The total number $\mathcal{N}_0$ of the Sturmians (17) coupled by the matrix-truncated proton-electron potential is equal to 45 927. Note that taking into account the attractive Coulomb potential $\hat{U}$ leads to a shift of the recoil peak in the forward direction by approximately 30°, whereas the position of the binary peak remains practically unchanged: it shifts in the opposite direction by about 3°. As indicated in Sec. II B, the splitting (12) in the Hamiltonian can be chosen differently. To explore this possibility, we have modified the final channel interaction by replacing the Coulomb potential $1/R$ for the proton and $-1/r$ for the electron by, respectively, the Hartree potentials for the (e^-, He$^+$) and (p^+, He$^+$) systems [20]. It can be seen from Fig. 3 that such S-wave short-range additions predictably do not affect the peak positions, but only slightly change their intensities.

B. Comparison with available theoretical and experimental data

We now turn to the comparison of our results with experiment and other theoretical calculations. We present in Fig. 4 the laboratory frame FDCSs in the case of $E_e = 6.5$ eV and $q = 0.75$ a.u. Theoretical values are obtained using our approach (CQS), the WP-CCC method [15] [multiplied by $(m_p/\mu)^2 = 25/16$], and the FBA and 3C model [14]. The experimental values are due to Ref. [4] with normalization of Ref. [14]. The theoretical FDCSs presented in Fig. 4 differ in the recoil/binary ratio and in the peaks' positions. In this respect, the FDCS calculated using our approach somewhat better agrees with the measured angular distribution. At the same time, common to all these theoretical approaches is their
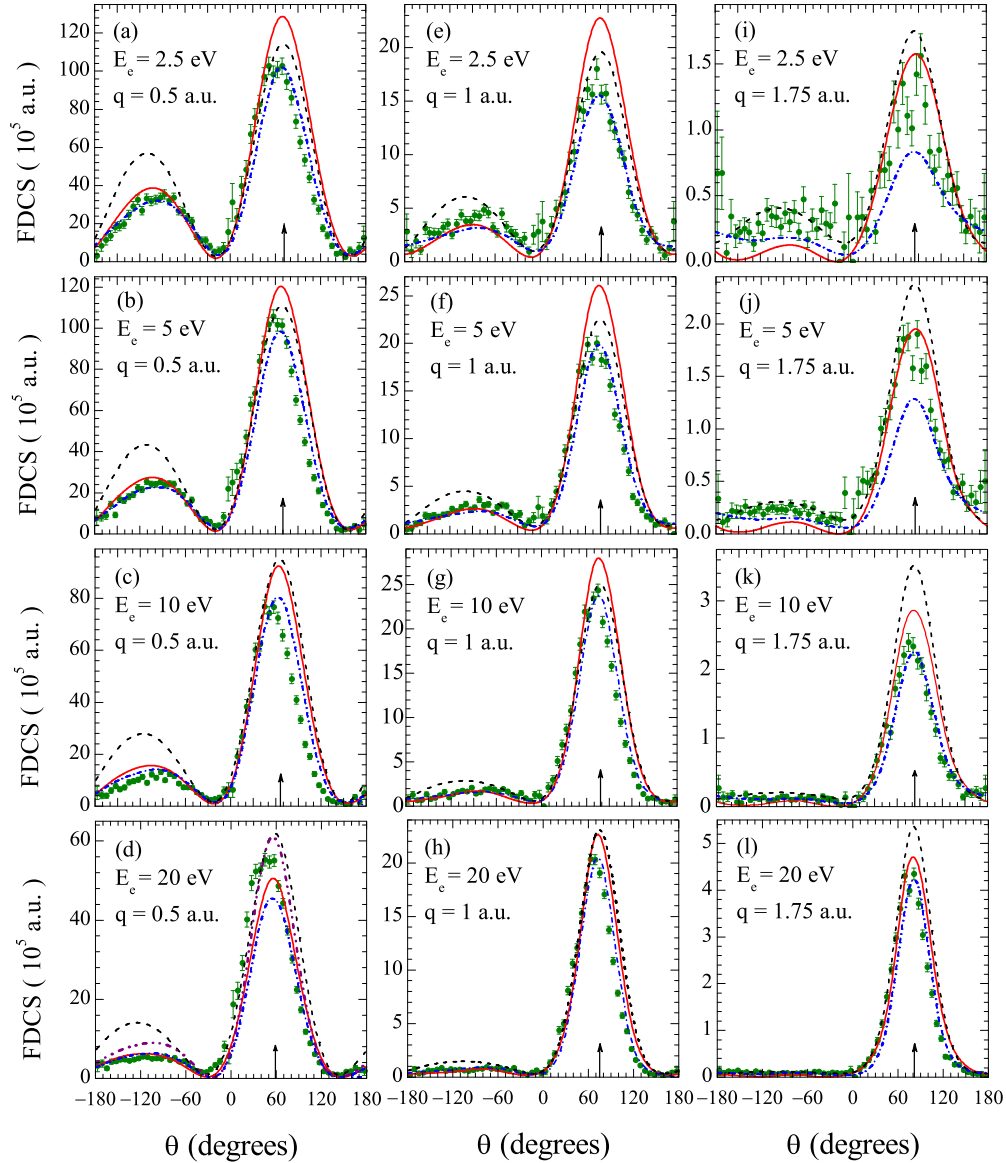
FIG. 5. FDCSs for single ionization of helium by 1-MeV protons in the collision plane in different kinematical regimes in the scattering plane. The ejected-electron energies and momentum transfer values are indicated in the legend. Solid curves show the results obtained with our method of convoluted quasi-Sturmians (CQS). Experiment is shown by solid circles with error bars, the FBA and 3C calculations (when available) by dashed and dotted lines, respectively, and the dash-dotted line represents the WP-CCC results.

inability to explain the experimental angular position of the binary peak; the discrepancy reaches $10°$, of which hardly $2°$ can be attributed to experimental uncertainties (see Fig. 9 of Ref. [5] and the relevant discussion therein).

To further test our approach, we calculated the FDCSs in the collision plane for the 12 sets of the E_e and q values considered in Ref. [5]. Our calculations are shown in Fig. 5 in comparison with experiment, and the FBA, 3C, and WP-CCC results. Three general features should be pointed out. First, the recoil/binary ratio obtained within our CQS approach agrees better with the WP-CCC results and experiment than those obtained within the FBA. Second, similarly to what we observed in Fig. 4, our CQS calculations yield practically the same binary-peak position as the 3C and WP-CCC approaches; this backs up the reliability of both our CQS approach and its numerical implementation. Third, the theoretical binary

peak in the kinematical regime where $E_e = 20$ eV and $q = 0.5$ a.u. is shifted by almost $10°$ towards larger angles with respect to the experimental one. As discussed in Ref. [5], this particular kinematical regime most strongly departs from the kinematics of the free proton-electron collision, or the Bethe ridge, and the corresponding FBA calculation most strongly disagrees with experiment. The $10°$ discrepancy between the more advanced theoretical calculations (3C, WP-CCC, and CQS) and experiment clearly indicates that the discussed theoretical treatments may miss some important ingredients of the ionization dynamics.

IV. SUMMARY

We have put forth a fully quantum-mechanical method for calculating fully differential cross sections for the proton-

impact ionization of helium. We calculate the transition amplitude as a sum of products of basis amplitudes associated to the asymptotic behavior of quasi-Sturmian basis functions in parabolic coordinates. In the framework of the frozen-core model, we transform the driven equation for the final-state three-body system $(e^-, \mathrm{He}^+, p^+)$ into a matrix equation, considering the proton-electron potential $\hat{U}$ as a perturbation. This algebraic approach is obtained by using Sturmian-expansion representations of the potential $\hat{U}$ and Green's function operator $\hat{G}_0^{(+)}$ of the two noninteracting hydrogenic subsystems (e^-, He^+) and (p^+, He^+). The matrix elements of the Green's functions are obtained in analytic form. This allows for an efficient calculation of their convolution and thus ensures a proper treatment of the energy spectrum of active electrons. In the considered high-energy limit the numerical method is robust in all kinematical situations explored; moreover, the method turns out to be numerically efficient since convergence of the cross sections is achieved with a moderate number of terms of the expansions. It should be noted that a single set of the coefficients $C_{\mathfrak{N}}$ (determined by the energy E and the difference $K_0 - Q$) is used in the calculations of all these cross sections. This feature demonstrates another advantage of our approach from the viewpoint of computational efficiency.

In spite of their diversity, none of the theoretical approaches proposed in the literature—including the present CQS—is capable of describing satisfactorily the binary-peak location in the measured electron angular distributions. At the same time, the differences between the theoretical results are insignificant compared to their discrepancy with the experimental data. Interestingly, the position of the binary peak (in contrast to the recoil peak) turns out to be practically insensitive to switching on or off the Coulomb proton-electron potential. This suggests that the discussed advanced quantum-mechanical treatments may miss some important feature of the binary-encounter mechanism, and therefore the development of more sophisticated methods and approaches is required. In this work, we tested a model of the Hartree potential for the projectile-ion and electron-ion interactions and found, in the considered high-energy regime, no appreciable effect on the cross section.

Note that one of the possible explanations for the marked discrepancy between theory and experiment might be the use of the frozen-core model for describing the residual helium ion in the final channel. This feature is common for our approach, the FBA and 3C calculations [5,14], and also for the WP-CCC approach [15,16], which uses of the frozen-core approximation for the ionization dynamics. Therefore, we have also analyzed the effects beyond the model of the frozen He^+ state in the final channel of the discussed process. For this purpose we have performed the FDCS calculations accounting for the polarization of the recoil-ion state in the presence of the slow ejected electron: the intensity and angular distribution of the electron are only marginally affected. Specifically, we have found that the magnitude of the perturbation of the electronic wave function $\psi_{1s}^{\mathrm{He}^+}$ induced by the dipole part of the polarization potential [31,32] is only a few percent. We plan to explore more advanced approaches of accounting for the electron correlations in the final channel. In particular, the full Green's function for the subsystem (e^-, He^+) can be obtained at any energy argument by solving the corresponding Lippmann-Schwinger equation, for example, using the Sturmian function (15) representation (in a fashion analogous to that presented in Ref. [33]). This enables one both to appropriately modify the wave function of the bound electron and to refine the asymptotic behavior of the ejected electron. We also intend to investigate further the effect of the short-range part of the projectile-target interaction. One lead would be to replace the pure Coulomb potential by screened or model potentials as done, e.g., in Ref. [6]. These improvements are probably necessary if one wishes to investigate ionization at lower incident proton energy ($E = 75$ keV), which provides further challenges; indeed, the calculated cross sections were seen [34] to be very sensitive to the details of the account for the interaction between the projectile and the target core.

Finally, we plan to apply our parabolic quasi-Sturmians approach to study proton- and antiproton-impact ionization of heavier atoms, still treated as one-electron targets.

APPENDIX A: ASYMPTOTIC BEHAVIOR OF THE SHIFTED QUASI-STURMIANS

In this Appendix, we derive the $X \to \infty$ asymptotic behavior of the quasi-Sturmian

$$\langle \mathbf{X} | \mathcal{Q}_{\mathbf{Q}, \mathfrak{l}}^{(+)} \rangle = \langle \mathbf{X} | \hat{G}_C^{(+)}(Z, M; \mathcal{E}) | \mathbf{Q} \rangle |\widetilde{\mathfrak{l}} \rangle, \tag{A1}$$

where the plane wave $\langle \mathbf{X} | \mathbf{Q} \rangle = e^{i\mathbf{Q} \cdot \mathbf{X}} = e^{i\frac{Q}{2}(\xi' - \eta')}$ since $\mathbf{Q}$ is along the $\hat{z}$ axis. For this purpose, we use the following expansion of the Coulomb Green's function kernel:

$$G_C^{(+)}(Z, M, P; \mathbf{X}, \mathbf{X}') = \frac{1}{2\pi} \sum_{\varkappa = -\infty}^{\infty} e^{i\varkappa(\phi - \phi')}$$
$$\times \mathcal{G}^{\lambda(+)}(Z, M, P; \xi, \eta; \xi', \eta'), \tag{A2}$$

where $\lambda = |\varkappa|$. After performing the trivial ϕ' integration, we are left with

$$\langle \mathbf{X} | \mathcal{Q}_{\mathbf{Q}, \mathfrak{l}}^{(+)} \rangle = \frac{e^{i\varkappa\phi}}{\sqrt{2\pi}} \int_0^\infty d\xi' \int_0^\infty d\eta'$$
$$\times \mathcal{G}^{\lambda(+)}(Z, M, P; \xi, \eta; \xi', \eta') e^{i\frac{Q}{2}(\xi' - \eta')} \varphi_n^\lambda(\xi') \varphi_m^\lambda(\eta'). \tag{A3}$$

The components $\mathcal{G}^{\lambda(+)}$ are expressed as the convolution integral (see Eq. (16) in Ref. [23])

$$\mathcal{G}^{\lambda(+)}(Z, M, P; \xi, \eta; \xi', \eta') = -2M\frac{P}{2\pi i} \int_{-\infty}^\infty d\tau$$
$$\times g^{(+)}(\tau; \xi, \xi') g^{(+)}(\beta - \tau; \eta, \eta'), \tag{A4}$$

where $\beta = \frac{MZ}{P}$ is the Sommerfeld parameter, and $g^{(+)}$ is given in terms of the Whittaker functions $\mathcal{M}$ and $\mathcal{W}$ [36],

$$
g^{(+)}(t;\, \rho, \rho') = \frac{\Gamma\left(\frac{1+\lambda}{2} + it\right)}{\Gamma(1+\lambda)} \frac{1}{(-iP\rho_<)^{\frac{1}{2}}} \mathcal{M}_{-it,\,\frac{\lambda}{2}}(-iP\rho_<)
$$
$$
\times \frac{1}{(-iP\rho_>)^{\frac{1}{2}}} \mathcal{W}_{-it,\,\frac{\lambda}{2}}(-iP\rho_>), \tag{A5}
$$

with $\rho_< = \min(\rho, \rho')$, $\rho_> = \max(\rho, \rho')$. Expressing the Whittaker functions in terms of the Kummer functions M and U [24], we have

$$
g^{(+)}(t;\, \rho, \rho') = \frac{\Gamma\left(\frac{1+\lambda}{2} + it\right)}{\Gamma(1+\lambda)} \frac{1}{(-iP\rho_<)^{\frac{1}{2}}} e^{iP\rho_</2}(-iP\rho_<)^{\frac{1+\lambda}{2}}
$$
$$
\times M\left(\frac{1+\lambda}{2} + it, 1+\lambda, -iP\rho_<\right)
$$
$$
\times \frac{1}{(-iP\rho_>)^{\frac{1}{2}}} e^{iP\rho_>/2}(-iP\rho_>)^{\frac{1+\lambda}{2}}
$$
$$
\times U\left(\frac{1+\lambda}{2} + it, 1+\lambda, -iP\rho_>\right). \tag{A6}
$$

We are interested in the physical asymptotic limit corresponding to $\xi \to \infty$ and ξ' bounded, so that $\rho_> = \xi$ and $\rho_< = \xi'$. Taking the leading term $U(a, b, z) \simeq z^{-a}$ of the $|z| \to \infty$ limit [24], we get

$$
g^{(+)}(\tau;\, \xi, \xi') \simeq \frac{\Gamma\left(\frac{1+\lambda}{2} + i\tau\right)}{\Gamma(1+\lambda)} \frac{e^{-px}}{(2px)^{1/2}}(2px)^{-i\tau} \frac{e^{-px'}}{(2px')^{1/2}}
$$
$$
\times (2px')^{\frac{1+\lambda}{2}} M\left(\frac{1+\lambda}{2} + i\tau, 1+\lambda, 2px'\right), \tag{A7}
$$

where we have set $p = -\frac{iP}{2b}$ and introduced the reduced variables $x = b\xi$, and $x' = b\xi'$. In the same way, the $\eta \to \infty$ and η' bounded limit of $g^{(+)}(\beta - \tau;\, \eta, \eta')$ is given by Eq. (A7), where we have to replace τ by $\beta - \tau$, x by $y = b\eta$, and x' by $y' = b\eta'$.

Inserting the convolution integral (A4) into Eq. (A3), using the asymptotic expressions of $g^{(+)}$, and reordering the three integrations, we find

$$
\langle \mathbf{X} | \mathcal{Q}_{\mathbf{Q},\mathfrak{t}}^{(+)} \rangle = -\frac{e^{i\varkappa\phi}}{\sqrt{2\pi}} 2M \frac{P}{2\pi i} \int_{-\infty}^{\infty} d\tau\, \mathcal{I}_n(\tau) \mathcal{J}_m(\tau), \tag{A8}
$$

where

$$
\mathcal{I}_n(\tau) = I_n\, \Gamma\left(\frac{1+\lambda}{2} + i\tau\right) \frac{e^{-px}}{(2px)^{1/2}}(2px)^{-i\tau}, \tag{A9}
$$

$$
\mathcal{J}_m(\tau) = J_m\, \Gamma\left(\frac{1+\lambda}{2} + i(\beta - \tau)\right) \frac{e^{-py}}{(2py)^{1/2}}(2py)^{-i(\beta-\tau)}. \tag{A10}
$$

The quantities I_n (respectively J_m) stand for the integrals on ξ' or equivalently x' (respectively η' or y'), which can be performed analytically. Making use of the explicit expression of the Laguerre basis elements (16) and setting $q = -\frac{iQ}{2b}$, we

have

$$
I_n = \frac{1}{\Gamma(1+\lambda)} \frac{(n+\lambda)!}{n!\lambda!} \sqrt{\frac{2bn!}{(n+\lambda)!}} \frac{1}{b}
$$
$$
\times \int_0^{\infty} dx' (2x')^{\frac{\lambda}{2}} (2px')^{\frac{\lambda}{2}} e^{-(1+p+q)x'}
$$
$$
\times M(-n, 1+\lambda, 2x') M\left(\frac{1+\lambda}{2} + i\tau, 1+\lambda, 2px'\right). \tag{A11}
$$

The integral is easily calculated using formula (f, 9) in Ref. [37],

$$
I_n = \frac{(n+\lambda)!}{n!\lambda!} \sqrt{\frac{2bn!}{(n+\lambda)!}} \frac{1}{b} \left[-\frac{1-(p+q)}{1+(p+q)}\right]^n
$$
$$
\times (4p)^{\frac{\lambda}{2}} [(1+(p+q))(1-(p-q))]^{-\frac{1+\lambda}{2}}
$$
$$
\times \left[\frac{1+(p+q)}{1-(p-q)}\right]^{i\tau} {}_2F_1\left(-n, \frac{1+\lambda}{2} + i\tau; 1+\lambda; z\right), \tag{A12}
$$

where $z = \frac{-4p}{(1-(p+q))(1-(p-q))}$. By replacing q by $-q$ and τ by $\beta - \tau$ we find similarly

$$
J_m = \frac{(m+\lambda)!}{m!\lambda!} \sqrt{\frac{2bm!}{(m+\lambda)!}} \frac{1}{b} \left[-\frac{1-(p-q)}{1+(p-q)}\right]^m
$$
$$
\times (4p)^{\frac{\lambda}{2}} [(1+(p-q))(1-(p+q))]^{-\frac{1+\lambda}{2}}
$$
$$
\times \left[\frac{1+(p-q)}{1-(p+q)}\right]^{i(\beta-\tau)}
$$
$$
\times {}_2F_1\left(-m, \frac{1+\lambda}{2} + i(\beta - \tau); 1+\lambda; z\right). \tag{A13}
$$

It remains to perform the integration (A8) over τ. In order to extract the argument τ that appears in the hypergeometric functions in Eqs. (A12) and (A13) we make use of the series expansion

$$
{}_2F_1\left(-n, \frac{1+\lambda}{2} + i\tau; 1+\lambda; z\right) = \frac{\Gamma(1+\lambda)}{\Gamma\left(\frac{1+\lambda}{2} + i\tau\right)}
$$
$$
\times \sum_{j=0}^{n} (-1)^j \frac{n!}{(n-j)!} \frac{\Gamma\left(\frac{1+\lambda}{2} + i\tau + j\right)}{\Gamma(1+\lambda+j)} \frac{z^j}{j!}. \tag{A14}
$$

Including the factor $\Gamma(\frac{1+\lambda}{2} + i\tau)$ from Eq. (A9) and $\frac{(n_1+\lambda)!}{n_1!\lambda!}$ from Eq. (A12), we obtain the result

$$
\Gamma\left(\frac{1+\lambda}{2} + i\tau\right) \frac{(n+\lambda)!}{n!\lambda!} {}_2F_1\left(-n, \frac{1+\lambda}{2} + i\tau; 1+\lambda; z\right)
$$
$$
= \sum_{\nu=0}^{n} c_\nu^{(n,\lambda)} z^\nu \Gamma\left(\frac{1+\lambda}{2} + i\tau + \nu\right), \tag{A15}
$$

where we recognize the coefficients $c_j^{(n,\lambda)}$ of the Laguerre polynomials expansion (29). Similarly, from Eq. (A13) and

the factor $\Gamma(\frac{1+\lambda}{2} + i(\beta - \tau))$, we get

$$\Gamma\left(\frac{1+\lambda}{2} + i(\beta - \tau)\right)\frac{(m+\lambda)!}{m!\lambda!}$$
$$\times \, _2F_1\left(-m, \frac{1+\lambda}{2} + i(\beta - \tau); 1 + \lambda; z\right)$$
$$= \sum_{\mu=0}^{m} c_\mu^{(m,\lambda)} z^\mu \, \Gamma\left(\frac{1+\lambda}{2} + i(\beta - \tau) + \mu\right). \quad (A16)$$

Introducing the notation

$$u = \alpha\frac{y}{x}, \quad \alpha = \frac{[1 - (p+q)^2]}{[1 - (p-q)^2]}, \quad (A17)$$

the rest of the τ-dependent part of the integrand takes the concise form

$$u^{i\tau} = \left[\frac{1 + (p+q)}{1 - (p-q)}\right]^{i\tau}\left[\frac{1 + (p-q)}{1 - (p+q)}\right]^{-i\tau}(2px)^{-i\tau}(2py)^{i\tau}. \quad (A18)$$

Collecting all τ-dependent terms, we may calculate the following integral:

$$\mathcal{L} = \frac{1}{2\pi}\int_{-\infty}^{\infty} d\tau\, \Gamma\left(\frac{1+\lambda}{2} + i\tau + \nu\right)$$
$$\times \Gamma\left(\frac{1+\lambda}{2} + i(\beta - \tau) + \mu\right)u^{i\tau}. \quad (A19)$$

With the change variable $i\tau = \sigma$, we immediately recognize the Meijer G function (p. 206 of Ref. [38]), namely,

$$\mathcal{L} = \frac{1}{2\pi i}\int_{-i\infty}^{i\infty} d\sigma\, \Gamma\left(\frac{1+\lambda}{2} + \nu + \sigma\right)$$
$$\times \Gamma\left(\frac{1+\lambda}{2} + i\beta + \mu - \sigma\right)u^\sigma \quad (A20)$$
$$= G_{1,1}^{1,1}\left(u\Big|_{b_1}^{a_1}\right), \quad (A21)$$

where $a_1 = \frac{1-\lambda}{2} - \nu$ and $b_1 = \frac{1+\lambda}{2} + i\beta + \mu$. Note that to these parameters a_1 and b_1 corresponds the contour (2) L in [38] (p. 207) from $-i\infty$ to $i\infty$, i.e., exactly our case. Making use of the simpler expression of the Meijer function with these parameters [39]

$$G_{1,1}^{1,1}\left(u\Big|_{b_1}^{a_1}\right) = \Gamma(1 + b_1 - a_1)u^{b_1}(u + 1)^{a_1 - b_1 - 1} \quad (A22)$$

we have

$$\mathcal{L} = \Gamma(i\beta + \lambda + \nu + \mu + 1)\left(\frac{u}{1+u}\right)^{i\beta}$$
$$\times \left(\frac{u}{(1+u)^2}\right)^{\frac{1+\lambda}{2}}\frac{u^\mu}{(1+u)^{\nu+\mu}}. \quad (A23)$$

Since we have performed all integrations we may now collect all terms. For convenience, in what follows we set

$$c = \cos\frac{\theta}{2}, \quad s = \sin\frac{\theta}{2}, \quad (A24)$$

so that

$$u = \alpha\frac{y}{x} = \alpha\frac{\eta}{\xi} = \alpha\frac{2X\sin^2\left(\frac{\theta}{2}\right)}{2X\cos^2\left(\frac{\theta}{2}\right)} = \alpha\frac{s^2}{c^2}. \quad (A25)$$

We make a number of algebraic simplifications:

(a) We write

$$z^\nu z^\mu \frac{u^\mu}{(1+u)^{\nu+\mu}} = \left[\frac{-4p}{[1 - (p+q)][1 - (p-q)]}\right.$$
$$\left.\times \frac{1}{c^2 + \alpha s^2}\right]^{\nu+\mu}(c^2)^\nu(\alpha s^2)^\mu. \quad (A26)$$

(b) We combine

$$\left(\frac{u}{(1+u)^2}\right)^{\frac{1+\lambda}{2}} = \left[\frac{1 - (p+q)^2}{1 - (p-q)^2}\right]^{\frac{1+\lambda}{2}}\frac{\left(\frac{\sin\theta}{2}\right)^{1+\lambda}}{(c^2 + \alpha s^2)^{1+\lambda}} \quad (A27)$$

with the factor $e^{-px}(2px)^{-1/2}$ from Eq. (A9) and $e^{-py}(2py)^{-1/2}$ from Eq. (A10) and also the factors

$$(4p)^{\frac{\lambda}{2}}[(1 + (p+q))(1 - (p-q))]^{-\frac{1+\lambda}{2}}, \quad (A28)$$

$$(4p)^{\frac{\lambda}{2}}[(1 + (p-q))(1 - (p+q))]^{-\frac{1+\lambda}{2}}, \quad (A29)$$

from, respectively, Eqs. (A12) and (A13), to obtain

$$\frac{e^{iPX}}{-2iPX}\frac{1}{4p}\left[\frac{4p}{[1 - (p-q)^2]}\frac{1}{c^2 + \alpha s^2}\right]^{1+\lambda}\left(\frac{\sin\theta}{2}\right)^\lambda. \quad (A30)$$

(c) We combine

$$\left(\frac{u}{1+u}\right)^{i\beta} \quad (A31)$$

from Eq. (A26) with

$$\left[\frac{1 + (p-q)}{1 - (p+q)}\right]^{i\beta} \quad (A32)$$

from the last line in Eq. (A13) and $(2py)^{-i\beta}$ from Eq. (A10), to obtain

$$\left[\frac{1 + (p+q)}{1 - (p-q)}\frac{1}{c^2 + \alpha s^2}\right]^{i\beta}e^{-\frac{\pi\beta}{2}}e^{-i\beta\ln(2PX)}. \quad (A33)$$

Collecting all intermediate results, the remaining multiplying factors, after some algebraic simplification we obtain the following asymptotic behavior:

$$\langle\mathbf{X}|\mathcal{Q}_{\mathbf{Q},\uparrow}^{(+)}\rangle \simeq -\frac{e^{i\varkappa\phi}}{\sqrt{2\pi}}M\frac{i}{P}\sqrt{\frac{n!}{(n+\lambda)!}}\left[-\frac{1 - (p+q)}{1 + (p+q)}\right]^n$$
$$\times \sqrt{\frac{m!}{(m+\lambda)!}}\left[-\frac{1 - (p-q)}{1 + (p-q)}\right]^m$$
$$\times \left[\frac{4p}{1 - (p-q)^2}\frac{1}{c^2 + \alpha s^2}\right]^{1+\lambda}\left(\frac{\sin\theta}{2}\right)^\lambda$$
$$\times \left[\frac{1 + (p+q)}{1 - (p-q)}\frac{1}{c^2 + \alpha s^2}\right]^{i\beta}e^{-\frac{\pi\beta}{2}}\frac{e^{iPX - i\beta\ln(2PX)}}{X}$$
$$\times \sum_{\nu=0}^{n}c_\nu^{(n,\lambda)}\sum_{\mu=0}^{m}c_\mu^{(m,\lambda)}\Gamma(i\beta + \lambda + \nu + \mu + 1)$$
$$\times \left[\frac{-4p}{[1 - (p+q)][1 - (p-q)]}\frac{1}{c^2 + \alpha s^2}\right]^{\nu+\mu}$$
$$\times (c^2)^\nu(\alpha s^2)^\mu. \quad (A34)$$

APPENDIX B: MATRIX ELEMENTS OF THE GREEN'S FUNCTION OPERATOR

In this Appendix we provide an analytical expression for the matrix element (40). First, inserting the expansion (A2)

and integrating over $0 \leqslant \phi, \phi' \leqslant 2\pi$ gives

$$\langle \widetilde{l} | \langle \mathbf{Q} | \hat{G}_C^{(+)}(Z, M; \mathcal{E}) | \mathbf{Q} \rangle | \widetilde{l'} \rangle = \delta_{\varkappa, \varkappa'} \, \mathfrak{S}_{n,m;n',m'}^{\lambda(+)}(Z, M; P, Q),$$

(B1)

where the "radial" part $\mathfrak{S}_{n,m;n',m'}^{\lambda(+)}$ is expressed in terms of the integral

$$\mathfrak{S}_{n,m;n',m'}^{\lambda(+)}(Z, M; P, Q) \equiv \int_0^\infty d\xi \int_0^\infty d\eta \int_0^\infty d\xi' \int_0^\infty d\eta' \varphi_n^\lambda(\xi) \varphi_m^\lambda(\eta) \, e^{-\frac{iQ}{2}(\xi - \eta)} \mathcal{G}^{\lambda(+)}(Z, M, P; \xi, \eta; \xi', \eta')$$
$$\times \, e^{\frac{iQ}{2}(\xi' - \eta')} \varphi_{n'}^\lambda(\xi') \varphi_{m'}^\lambda(\eta').$$

(B2)

We then make use of the integral representation (see, e.g., Ref. [23])

$$\mathcal{G}^{\lambda(\pm)}(Z, M; P; \xi, \eta; \xi', \eta') = \pm iMP \int_0^\infty dz \, \sinh z \left(\coth \frac{z}{2} \right)^{\mp 2i\beta} e^{\pm i \frac{P}{2}(\xi + \xi' + \eta + \eta') \cosh z} I_\lambda(\mp iP\sqrt{\xi \xi'} \sinh z) I_\lambda(\mp iP\sqrt{\eta \eta'} \sinh z)$$

(B3)

and proceed by performing first the integration over ξ, ξ', η, and η'. We introduce the following convenient notation: $x = b\xi$, $y = b\eta$, $x' = b\xi'$, $y' = b\eta'$, $p = -\frac{iP}{2b}$, $q = -\frac{iQ}{2b}$, and $s = \sinh(z)$, $c = \cosh z$. Using the explicit form of the Laguerre basis functions φ_n^λ [Eq. (16)], the integrals over ξ, ξ' (respectively η, η') become

$$B_1 = \frac{2}{b} \sqrt{\frac{n! n'!}{(n + \lambda)! (n' + \lambda)!}} \int_0^\infty dx' \, e^{-(1 + pc + q)x'} (2x')^{\frac{\lambda}{2}} L_{n'}^\lambda(2x') \int_0^\infty dx \, e^{-(1 + pc - q)x} (2x)^{\frac{\lambda}{2}} L_n^\lambda(2x) I_\lambda(2p\sqrt{xx'}s) \quad (B4)$$

$$B_2 = \frac{2}{b} \sqrt{\frac{m! m'!}{(m + \lambda)! (m' + \lambda)!}} \int_0^\infty dy' \, e^{-(1 + pc - q)y'} (2y')^{\frac{\lambda}{2}} L_{m'}^\lambda(2y') \int_0^\infty dy \, e^{-(1 + pc + q)y} (2y)^{\frac{\lambda}{2}} L_m^\lambda(2y) I_\lambda(2p\sqrt{yy'}s). \quad (B5)$$

The integral in the second line of Eq. (B4), named hereafter $\mathcal{I}_1$, is calculated using formula (2.19.12, 6) of Ref. [40]:

$$\mathcal{I}_1 = (-1)^n \frac{(1 - [pc - q])^n}{(1 + [pc - q])^{n + \lambda + 1}} (ps\sqrt{2x'})^\lambda \exp\left(\frac{ps^2 x'}{1 + [pc - q]} \right) L_n^\lambda \left(\frac{-2p^2 s^2 x'}{1 - [pc - q]^2} \right),$$

(B6)

so that B_1 becomes

$$B_1 = \frac{2}{b} \sqrt{\frac{n! n'!}{(n + \lambda)! (n' + \lambda)!}} (-1)^n \frac{(1 - [pc - q])^n}{(1 + [pc - q])^{n + \lambda + 1}} (2ps)^\lambda \mathcal{I}_2,$$

(B7)

where it remains to perform the integration over x':

$$\mathcal{I}_2 = \int_0^\infty dx' \, x'^\lambda \exp\left\{ -x' \left(1 + pc + q - \frac{ps^2}{1 + [pc - q]} \right) \right\} L_{n'}^\lambda(2x') L_n^\lambda \left(\frac{-2p^2 s^2 x'}{1 - [pc - q]^2} \right).$$

(B8)

The latter is calculated using formula (2.19.14, 6) of Ref. [40], to obtain

$$\mathcal{I}_2 = \frac{(\lambda + 1)_{n'} (\lambda + 1)_n \Gamma(\lambda + 1)}{n'! \, n!} \frac{(-1)^{n'} \left(\frac{1 - p^2 + q^2 - 2q}{1 + [pc - q]} \right)^{n'} \left(\frac{1 - p^2 + q^2 + 2q}{1 - [pc - q]} \right)^n}{\left(\frac{1 + p^2 - q^2 + 2pc}{1 + [pc - q]} \right)^{n' + n + \lambda + 1}}$$
$$\times \, {}_2F_1\left(-n, -n', \lambda + 1; \frac{4p^2 s^2}{(1 - p^2 + q^2 - 2q)(1 - p^2 + q^2 + 2q)} \right).$$

(B9)

Further, inserting Eq. (B9) in Eq. (B7) gives

$$B_1 = \frac{2}{b} \sqrt{\binom{n' + \lambda}{n'} \binom{n + \lambda}{n}} \frac{(2ps)^\lambda}{(1 + p^2 - q^2 + 2pc)^{\lambda + 1}} \left(-\frac{1 - p^2 + q^2 - 2q}{1 + p^2 - q^2 + 2pc} \right)^{n'} \left(-\frac{1 - p^2 + q^2 + 2q}{1 + p^2 - q^2 + 2pc} \right)^n$$
$$\times \, {}_2F_1\left(-n, -n', \lambda + 1; \frac{4p^2 s^2}{(1 - p^2 + q^2 - 2q(1 - p^2 + q^2 + 2q)} \right),$$

(B10)

and similarly

$$B_2 = \frac{2}{b} \sqrt{\binom{m'+\lambda}{m'}\binom{m+\lambda}{m}} \frac{(2ps)^\lambda}{(1+p^2-q^2+2pc)^{\lambda+1}} \left(-\frac{1-p^2+q^2+2q}{1+p^2-q^2+2pc}\right)^{m'} \left(-\frac{1-p^2+q^2-2q}{1+p^2-q^2+2pc}\right)^m$$

$$\times \,_2F_1\left(-m,-m',\lambda+1; \frac{4p^2s^2}{(1-p^2+q^2+2q)(1-p^2+q^2-2q)}\right). \tag{B11}$$

Then we use the notation

$$t = \left[\tanh\left(\frac{z}{2}\right)\right]^2, \tag{B12}$$

$$\zeta = \chi\delta, \quad \chi = \frac{1-(p+q)}{1+(p+q)}, \quad \delta = \frac{1-(p-q)}{1+(p-q)}, \tag{B13}$$

to write

$$1 + p^2 - q^2 + 2p = \frac{4p}{(1-\zeta)},$$

$$1 + p^2 - q^2 + 2pc = \frac{4p}{(1-\zeta)} \frac{(1-\zeta t)}{(1-t)},$$

$$1 - p^2 + q^2 - 2q = \frac{4p}{(1-\zeta)} \chi,$$

$$1 - p^2 + q^2 + 2q = \frac{4p}{(1-\zeta)} \delta, \tag{B14}$$

and therefore

$$B_1 = \frac{1}{2pb} \sqrt{\binom{n+\lambda}{n}\binom{n'+\lambda}{n'}} (1-\zeta)^{\lambda+1}(-\chi)^{n'}(-\delta)^n$$

$$\times t^{\lambda/2}(1-t)^{n+n'+1}(1-\zeta t)^{-(n+n'+\lambda+1)}$$

$$\times \,_2F_1\left(-n,-n',\lambda+1; \frac{(1-\zeta)^2}{\zeta}\frac{t}{(1-t)^2}\right), \tag{B15}$$

$$B_2 = \frac{1}{2pb} \sqrt{\binom{m+\lambda}{m}\binom{m'+\lambda}{m'}} (1-\zeta)^{\lambda+1}(-\chi)^m(-\delta)^{m'}$$

$$\times t^{\lambda/2}(1-t)^{m+m'+1}(1-\zeta t)^{-(m+m'+\lambda+1)}$$

$$\times \,_2F_1\left(-m,-m',\lambda+1; \frac{(1-\zeta)^2}{\zeta}\frac{t}{(1-t)^2}\right). \tag{B16}$$

All that remains is to calculate the integral over z in Eq. (B3). Naming $\mathcal{J}_{n,n'}$ and $\mathcal{J}_{m,m'}$ the products of the two last lines of Eqs. (B15) and (B16), respectively, the radial part becomes $\mathfrak{S}_{n,m;n',m'}^{\lambda(+)}(Z,M;P,Q) = C\mathcal{K}$ where

$$C = \frac{1}{4p^2b^2} \sqrt{\binom{n+\lambda}{n}\binom{n'+\lambda}{n'}\binom{m+\lambda}{m}\binom{m'+\lambda}{m'}}$$

$$\times (1-\zeta)^{2\lambda+2}(-\delta)^{n+m'}(-\chi)^{m+n'} \tag{B17}$$

and

$$\mathcal{K} = iMP \int_0^\infty dz \, \sinh(z) \left[\coth\left(\frac{z}{2}\right)\right]^{-2i\beta} \mathcal{J}_{n,n'} \mathcal{J}_{m,m'}. \tag{B18}$$

To proceed analytically it is convenient to use the change of variables

$$t = \left[\tanh\left(\frac{z}{2}\right)\right]^2 \Rightarrow dt = \sqrt{t}(1-t)dz \tag{B19}$$

to write

$$\mathcal{K} = 2iMP \int_0^1 dt \, t^{i\beta+\lambda}(1-t)^L(1-\zeta t)^{-L-2\lambda-2}$$

$$\times \,_2F_1\left(-n,-n',\lambda+1; \frac{(1-\zeta)^2}{\zeta}\frac{t}{(1-t)^2}\right)$$

$$\times \,_2F_1\left(-m,-m',\lambda+1; \frac{(1-\zeta)^2}{\zeta}\frac{t}{(1-t)^2}\right), \tag{B20}$$

where

$$L = n + n' + m + m'. \tag{B21}$$

Further, similarly to what was done in Appendix A of Ref. [23], we express the product of the two hypergeometric functions as a polynomial (for convenience, we provide here the full derivation)

$$\sum_{\ell=0}^{u+v} c_\ell \left[\frac{(1-\zeta)^2}{\zeta}\frac{t}{(1-t)^2}\right]^\ell, \tag{B22}$$

whose coefficients c_ℓ are

$$c_\ell = \sum_{j=\max(\ell-v,0)}^{\min(\ell,u)} \frac{\binom{n}{j}\binom{n'}{j}\binom{m}{\ell-j}\binom{m'}{\ell-j}}{\binom{j+\lambda}{j}\binom{\ell-j+\lambda}{\ell-j}},$$

with $u = \min(n,n')$ and $v = \min(m,m')$. We thus express Eq. (B20)

$$\mathcal{K} = 2iMP \sum_{\ell=0}^{u+v} c_\ell \frac{(1-\zeta)^{2\ell}}{\zeta^\ell} \mathcal{L}_\ell \tag{B23}$$

in terms of the integrals

$$\mathcal{L}_\ell = \int_0^1 dt \, t^{i\beta+\lambda+\ell}(1-t)^{L-2\ell}(1-\zeta t)^{-L-2\lambda-2}, \tag{B24}$$

which are readily identified as the integral representation of Gauss hypergeometric functions (Eq. (15.3.1) of Ref. [24])

$$\mathcal{L}_\ell = \frac{\Gamma(i\beta+\lambda+\ell+1)\Gamma(L-2\ell+1)}{\Gamma(i\beta+L+\lambda+2-\ell)}$$

$$\times \,_2F_1(L+2\lambda+2,\lambda+\ell+1+i\beta; L+\lambda++2-\ell+i\beta;\zeta)$$

$$= \frac{1}{(1-\zeta)^{2\lambda+1+2\ell}} \frac{\Gamma(i\beta+\lambda+\ell+1)\Gamma(L-2\ell+1)}{\Gamma(i\beta+L+\lambda+2-\ell)}$$

$$\times \,_2F_1(L-2\ell+1,-\lambda-\ell+i\beta; L+\lambda+2-\ell+i\beta;\zeta), \tag{B25}$$

the second equality being obtained through the transformation (15.3.3) of Ref. [24].

Finally, inserting Eq. (B25) in Eq. (B23), we obtain a representation for the integrals (B20) which, multiplied by C

defined by Eq. (B17), gives the matrix element (B1) in the form of the finite sum (40). In the absence of the plane wave, i.e., when $Q = 0$, this result was presented in Appendix A of Ref. [23].

[1] R. Dörner, V. Mergel, O. Jagutzki, L. Spielberger, J. Ullrich, R. Moshammer, and H. Schmidt-Böcking, Phys. Rep. **330**, 95 (2000).

[2] J. Ullrich, R. Moshammer, A. Dorn, R. Dörner, L. Ph. H. Schmidt, and H. Schmidt-Böcking, Rep. Prog. Phys. **66**, 1463 (2003).

[3] J. Ullrich, R. Moshammer, R. Dörner, O. Jagutzki, V. Mergel, H. Schmidt-Böcking, and L. Spielberger, J. Phys. B **30**, 2917 (1997).

[4] H. Gassert, O. Chuluunbaatar, M. Waitz, F. Trinter, H.-K. Kim, T. Bauer, A. Laucke, C. Müller, J. Voigtsberger, M. Weller, J. Rist, M. Pitzer, S. Zeller, T. Jahnke, L. Ph. H. Schmidt, J. B. Williams, S. A. Zaytsev, A. A. Bulychev, K. A. Kouzakov, H. Schmidt-Böcking *et al.*, Phys. Rev. Lett. **116**, 073201 (2016).

[5] O. Chuluunbaatar, K. A. Kouzakov, S. A. Zaytsev, A. S. Zaytsev, V. L. Shablov, Yu. V. Popov, H. Gassert, M. Waitz, H.-K. Kim, T. Bauer, A. Laucke, Ch. Müller, J. Voigtsberger, M. Weller, J. Rist, K. Pahl, M. Honig, M. Pitzer, S. Zeller, T. Jahnke, L. Ph. H. Schmidt *et al.*, Phys. Rev. A **99**, 062711 (2019).

[6] L. Sarkadi, Phys. Rev. A **97**, 042703 (2018).

[7] D. Belkic, R. Gayet, and A. Salin, Phys. Rep. **56**, 279 (1979).

[8] D. S. F. Crothers and L. J. Dube, Adv. At. Mol. Opt. Phys. **30**, 287 (1993).

[9] A. B. Voitkiv, Phys. Rev. A **95**, 032708 (2017).

[10] A. Igarashi and L. Gulyás, J. Phys. B: At. Mol. Opt. Phys. **52**, 245203 (2019).

[11] S. Amiri Bidvari and R. Fathi, Eur. Phys. J. Plus **136**, 190 (2021); **136**, 453 (2021).

[12] C. R. Garibotti and J. E. Miraglia, Phys. Rev. A **21**, 572 (1980).

[13] M. Brauner, J. S. Briggs, and H. Klar, J. Phys. B **22**, 2265 (1989).

[14] O. Chuluunbaatar, S. A. Zaytsev, K. A. Kouzakov, A. Galstyan, V. L. Shablov, and Yu. V. Popov, Phys. Rev. A **96**, 042716 (2017).

[15] I. B. Abdurakhmanov, A. S. Kadyrov, I. Bray, and K. Bartschat, Phys. Rev. A **96**, 022702 (2017).

[16] I. B. Abdurakhmanov, A. S. Kadyrov, Sh. U. Alladustov, I. Bray, and K. Bartschat, Phys. Rev. A **100**, 062708 (2019).

[17] G. S. Was, *Fundamentals of Radiation Materials Science* (Springer-Verlag, New York, 2017).

[18] *Ion Beam Therapy*, edited by U. Linz (Springer-Verlag, Berlin, 2012).

[19] H.-K. Kim, J. Titze, M. Schöffler, F. Trinter, M. Waitz, J. Voigtsberger, H. Sann, M. Meckel, C. Stuck, U. Lenz, D.

Metz, A. Jung, M. Odenweller, N. Neumann, S. Schössler, K. Ullmann-Pfleger, B. Ulrich, R. Costa Fraga, N. Petridis, D. Metz *et al.*, Proc. Natl. Acad. Sci. USA **108**, 11821 (2011).

[20] S. A. Zaytsev, A. S. Zaytsev, V. V. Nasyrov, D. S. Zaytseva, L. U. Ancarani, and K. A. Kouzakov, Atoms **10**, 13 (2022).

[21] S. P. Merkuriev and L. D. Faddeev, *Quantum Scattering Theory for Several Particle Systems* (Kluwer Academic, Dordrecht, 1993).

[22] A. Messiah, *Quantum Mechanics* (North-Holland, Amsterdam, 1966), Vol. 2.

[23] S. A. Zaytsev, L. U. Ancarani, A. S. Zaytsev, and K. A. Kouzakov, Eur. Phys. J. Plus **135**, 655 (2020).

[24] *Handbook of Mathematical Functions with Formulas, Graphs, and Mathematical Tables, 9th printing*, edited by M. Abramowitz and I. A. Stegun (Dover, New York, 1972).

[25] A. S. Zaytsev, L. U. Ancarani, and S. A. Zaytsev, Eur. Phys. J. Plus **131**, 48 (2016).

[26] A. Baz, Ya. Zeldovich, and A. Perelomov, *Scattering, Reactions, and Decays, in Nonrelativistic Quantum Mechanics* (Nauka, Moscow, 1966).

[27] R. Shakeshaft, Phys. Rev. A **70**, 042704 (2004).

[28] A. S. Zaytsev, D. S. Zaytseva, L. U. Ancarani, and S. A. Zaytsev, Eur. Phys. J. D **73**, 111 (2019).

[29] M. J. Ambrosio, F. D. Colavecchia, G. Gasaneo, D. M. Mitnik, and L. U. Ancarani, J. Phys. B **48**, 055204 (2015).

[30] O. Chuluunbaatar, I. V. Puzynin, P. S. Vinitsky, Yu. V. Popov, K. A. Kouzakov, and C. Dal Cappello, Phys. Rev. A **74**, 014703 (2006).

[31] R. M. Sternheimer, Phys. Rev. **96**, 951 (1954).

[32] A. K. Bhatia and A. Temkin, Phys. Rev. A **64**, 032709 (2001).

[33] S. A. Zaytsev, V. A. Knyr, Yu. V. Popov, and A. Lahmam-Bennani, Phys. Rev. A **75**, 022718 (2007).

[34] L. Gulyás, S. Egri, and A. Igarashi, Phys. Rev. A **99**, 032704 (2019).

[35] A. A. Sorokin, S. V. Makogonov, and S. P. Korolev, Sci. Tech. Inf. Process. **44**, 302 (2017).

[36] R. G. Newton, *Scattering Theory of Waves and Particles* (McGraw-Hill, New-York, 1966).

[37] L. D. Landau and E. M. Lifshitz, *Quantum Mechanics (Nonrelativistic Theory)* (Pergamon, Oxford, UK, 1977).

[38] H. Bateman and A. Erdélyi, *Higher Transcendental Functions Volume I* (McGraw-Hill, New York, 1953).

[39] Wolfram formula, https://functions.wolfram.com/HypergeometricFunctions/MeijerG/03/01/03/11/.

[40] A. P. Prudnikov, Yu. A. Brychkov, and O. I. Marichev, *Integrals and Series. Volume 2: Special Functions* (Gordon and Breach, New York, 1992).